

# Theoretical prediction of the nondiffractive propagation of sonic waves through periodic acoustic media

Isabel Pérez-Arjona,<sup>1</sup> Víctor J. Sánchez-Morcillo,<sup>1</sup> Javier Redondo,<sup>1</sup> Víctor Espinosa,<sup>1</sup> and Kestutis Staliunas<sup>2</sup>

<sup>1</sup>*Departamento de Física Aplicada, Escuela Politécnica Superior de Gandia, Universidad Politécnica de Valencia, Ctra. Nazaret-Oliva s/n, 46730 Grau de Gandia, Spain*

<sup>2</sup>*ICREA, Departament de Física i Enginyeria Nuclear, Universitat Politècnica de Catalunya, Colom 11, E-08222 Terrassa, Barcelona, Spain*

(Received 15 June 2006; revised manuscript received 2 November 2006; published 22 January 2007)

We predict theoretically the nondiffractive propagation of sonic waves in periodic acoustic media (sonic crystals) by expansion into a set of plane waves (Bloch mode expansion) and by finite-difference time-domain calculations of finite beams. We also give analytical evaluations of the parameters for nondiffractive propagation, as well as the minimum size of the nondiffractively propagating acoustic beams.

DOI: [10.1103/PhysRevB.75.014304](https://doi.org/10.1103/PhysRevB.75.014304)

PACS number(s): 43.20.+g, 43.35.+d.

## I. INTRODUCTION

The study of the dynamics of waves, even in simple linear media, initiated hundreds of year ago, ever and ever leads to surprisingly new results and insights. One of such “surprises” was the discovery of band gaps in the propagation of light in materials with the refraction index periodically modulated on the scale of the optical wavelength, the so-called photonic crystals.<sup>1</sup> The theory of wave propagation in periodic materials was developed a long time ago by Bloch and Floquet, and it found many applications in solid-state physics, in particular in the studies of electronic properties of semiconductors (calculation of valence and conduction bands, etc.). Nevertheless, the advent of photonic crystals initiated a revival of the theory of wave propagation in periodic media. The creation and control of photonic band gaps,<sup>2</sup> the slowing down of light,<sup>3</sup> and the photonic crystal waveguides are the main applications to date. Most of these studies concern the propagation of plane waves (not beams) and result in a modification of the *temporal* dispersion relation (frequency versus propagation wavenumber). Later, strong analogies between the propagation of light and sound (which obey similar wave equations) motivated the study of sound propagation in periodic acoustic media, the so-called sonic or phononic crystals (SC’s). Many of the results obtained in the photonic case have been reported in the sonic case. For a review on this topic, see, e.g., Ref. 4.

Most of the studies reported above concern one-dimensional (1D) periodic structures, as the 1D case, being relatively simple, allows an analytical treatment. The multidimensional cases (the 2D case as in our present study or even the 3D case) are much more difficult to be accessed analytically. The majority of these studies in the multidimensional case are numeric, as using plane-wave expansion, or finite-difference time-domain (FDTD) schemes. These studies also mostly concern the modification of the *temporal* dispersion characteristics.

It has come out recently that the spatial periodicity can affect not only temporal dispersion, but also the *spatial* one—i.e., the dependence of the longitudinal component of the propagation constant versus the transverse component. These results (again predominantly numeric) lead to the so-

called management of spatial dispersion—i.e., to the management of diffraction properties of narrow beams. This idea led to a prediction of the negative diffraction of light beams in photonic crystals,<sup>5</sup> of sound beams in sonic crystals,<sup>6</sup> and of coherent atomic ensembles in Bose-Einstein condensates in periodic potentials.<sup>7</sup> In particular it has been found recently that between the normal diffraction and negative diffraction regimes a strong reduction of the diffraction can be achieved, leading to the so-called self-collimating, or nondiffractive light beams. These studies consist of the initial proposal of the idea of self-collimation,<sup>8</sup> of its experimental demonstration,<sup>8,9</sup> the issues of light coupling to the self-collimating crystal,<sup>10</sup> the calculation of asymptotic (long-distance) properties of the propagation of self-collimated light,<sup>11</sup> and others.

The geometrical interpretation of wave diffraction is as follows: wave beams of arbitrary shape can be Fourier decomposed into plane waves, which in propagation acquire phase shifts depending on their propagation angles. This dephasing of the plane-wave components results in a diffractive broadening of the beams. Figure 1(a) illustrates normal diffraction in propagation through an homogeneous material, where the longitudinal component of the wave vector depends trivially on the propagation angle,  $k_{\parallel} = k_z = \sqrt{|\mathbf{k}|^2 - |\mathbf{k}_{\perp}|^2}$ , where  $\mathbf{k}_{\perp} = (k_x, k_y)$ . In general, the normal or positive diffraction means that the surfaces of constant frequency are concave in the wave vector domain  $\mathbf{k} = (k_x, k_y, k_z)$ , as illustrated in Fig. 1(a). The negative diffraction, as illustrated in Fig. 1(b), geometrically means that the

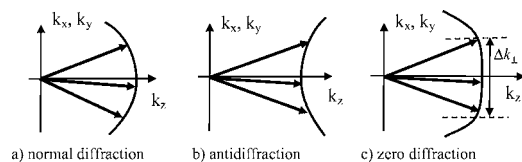


FIG. 1. Geometrical interpretation of diffraction of waves propagating along the  $z$  axis: (a) positive, or normal diffraction in propagation through homogeneous materials; (b) negative, or anomalous diffraction; (c) zero diffraction. The area of negligible diffraction (for evaluation of the minimum size of the nondiffractive beam) is indicated.

surfaces of constant frequency are convex in the wave vector domain. The intermediate case of the vanishing diffraction is illustrated in Fig. 1(c), where the zero diffraction is supposed to occur at a particular point in the wave vector domain where the curvature of the surfaces of constant frequency becomes exactly zero. Zero diffraction physically means that beams of arbitrary width can propagate without diffractive broadening or, equivalently, that arbitrary wave structures can propagate without diffractive “smearing.”

The present study concerns the nondiffractive propagation of sound in periodic acoustic materials (sonic crystals). We found, by applying the plane-wave expansion method, the existence of nondiffractive regimes similar to those in optics, or to those expected from Fig. 1(c). We check the nondiffractive propagation by integrating the wave equations by means of the FDTD technique. Moreover, we also present an analytical treatment of the problem, leading to analytic relations, which among others are useful for the planning of the corresponding experiment and for designing the possible applications.

In Sec. II of the article the propagation of sound is analyzed by plane-wave expansion, leading to the spatial dispersion curves and in particular resulting in straight (nondiffractive) segments of the spatial dispersion curves. In this way the nondiffractive propagation regimes are predicted. In the next section III the FDTD calculations are performed in the predicted nondiffractive regimes and the nonspreading propagation of narrow beams is demonstrated. Section IV is devoted to the analytical study, to the derivation of analytical relations between parameters for the nondiffractive propagation. The last section contains the concluding remarks, where the results are summarized and also the minimal size of the beams propagating nondiffractively is evaluated.

## II. DISPERSION IN SONIC CRYSTALS

The propagation of sonic waves is determined by the following linear system equations:

$$\rho \frac{\partial \mathbf{v}}{\partial t} = -\nabla p, \quad (1a)$$

$$\frac{\partial p}{\partial t} = -B \nabla \cdot \mathbf{v}, \quad (1b)$$

where  $B(\mathbf{r})$  is the bulk modulus,  $\rho(\mathbf{r})$  is the density (both dependent in space),  $p(\mathbf{r}, t)$  is the pressure (which are scalar fields), and  $\mathbf{v}(\mathbf{r}, t)$  is the velocity vector field.

We define the relative values of the bulk modulus  $\bar{B}(\mathbf{r}) = B(\mathbf{r})/B_h$  and the density  $\bar{\rho}(\mathbf{r}) = \rho(\mathbf{r})/\rho_h$ , normalizing to the corresponding parameters in the host medium. Then, eliminating the velocity field in Eqs. (1), we obtain a wave equation describing the propagation of sound in the inhomogeneous medium,

$$\frac{1}{\bar{B}(\mathbf{r})} \frac{\partial^2 p(\mathbf{r}, \tau)}{\partial \tau^2} - \nabla \cdot \left( \frac{1}{\bar{\rho}(\mathbf{r})} \nabla p(\mathbf{r}, \tau) \right) = 0, \quad (2)$$

where  $\tau = c_h t$  is a normalized time, which makes the velocity of sound in the host medium  $c_h$  equal to unity, where  $c_h = \sqrt{B_h/\rho_h}$ .

We consider sound beams with harmonic temporal dependence. Then, the steadily oscillating solution has the form  $p(\mathbf{r}, t) = p(\mathbf{r})e^{i\omega\tau}$ , which substituted in Eq. (2) leads to the eigenvalue equation

$$\frac{\omega^2}{\bar{B}(\mathbf{r})} p(\mathbf{r}) + \nabla \cdot \left( \frac{1}{\bar{\rho}(\mathbf{r})} \nabla p(\mathbf{r}) \right) = 0. \quad (3)$$

For the subsequent analysis we consider a concrete geometry, where acoustic waves propagate in a two-dimensional medium, formed by an squared array of solid cylinders, with the axis along the  $y$  direction and radius  $r_0$ , in a host fluid medium. The coordinate  $\mathbf{r}$  in Eq. (3) depends now on longitudinal ( $z$ ) and transverse ( $x$ ) directions, and  $\nabla = (\partial/\partial x, \partial/\partial z)$ .

The lattice defined though the centers of cylinders is given by the set  $R = \{\mathbf{R} = n_1 \mathbf{a}_1 + n_2 \mathbf{a}_2; n_1, n_2 \in N\}$  of two-dimensional lattice vectors  $\mathbf{R}$ , which are generated by the primitive translations  $\mathbf{a}_1$  and  $\mathbf{a}_2$ . The corresponding reciprocal lattice is defined though  $G = \{\mathbf{G} : \mathbf{G} \cdot \mathbf{R} = 2\pi n; n \in N\}$ .

A possible way of solving Eq. (3) is by means of the plane-wave expansion (PWE) method, which converts the differential equation into an infinite matrix eigenvalue problem, which is then truncated and solved numerically. By solving this eigenvalue problem the frequencies corresponding to each Bloch wave can be obtained, providing the dispersion relationship and band structure of the periodic medium.

The bulk modulus and density are periodic functions with the periodicity of the lattice and therefore contain all the information of the phononic crystal. This implies that the material parameters can be represented by their Fourier expansions on the basis of the reciprocal lattice,

$$\bar{\rho}(\mathbf{r})^{-1} = \sum_{\mathbf{G}} \rho_{\mathbf{G}}^{-1} e^{i\mathbf{G} \cdot \mathbf{r}}, \quad (4)$$

$$\bar{B}(\mathbf{r})^{-1} = \sum_{\mathbf{G}} b_{\mathbf{G}}^{-1} e^{i\mathbf{G} \cdot \mathbf{r}}. \quad (5)$$

On the other hand, the solutions  $p(\mathbf{r})$  of Eq. (3) must be also periodic with the periodicity of the lattice (Bloch-Floquet theorem) and can be expanded as

$$p(\mathbf{r}) = e^{i\mathbf{k} \cdot \mathbf{r}} \sum_{\mathbf{G}} p_{\mathbf{k}, \mathbf{G}} e^{i\mathbf{G} \cdot \mathbf{r}}, \quad (6)$$

where  $\mathbf{k}$  is a two-dimensional Bloch vector restricted to the first Brillouin zone and  $\mathbf{G}$  denotes a reciprocal lattice vector. For a square lattice,  $\mathbf{G} = (2\pi/a)(n_1 \mathbf{e}_1 + n_2 \mathbf{e}_2)$  with  $n_1$  and  $n_2$  integers and  $a$  being the lattice constant (minimal distance between the centers of neighbor cylinders).

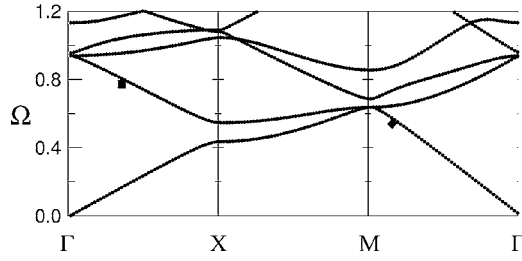


FIG. 2. Band structure for steel cylinders in water, for  $r = 1$  mm and  $a = 5.25$  mm, as calculated by the expansion into Bloch modes (4)–(7). The solid squares mark the nondiffractive points (see Fig. 3).

The coefficients in expansions (4) and (5) can be obtained from the inverse Fourier transform. For the inverse of mass density the coefficients result<sup>12</sup>

$$\rho_{\mathbf{G}}^{-1} = \frac{1}{a^2} \int_U \int_C \frac{1}{\bar{\rho}(\mathbf{r})} d\mathbf{r} = \frac{\rho_h}{\rho_c} f + (1-f), \quad \text{for } \mathbf{G} = 0, \quad (7)$$

which represents the average value of the density, and

$$\rho_{\mathbf{G}}^{-1} = \frac{1}{a^2} \int_U \int_C \frac{e^{i\mathbf{G}\cdot\mathbf{r}}}{\bar{\rho}(\mathbf{r})} d\mathbf{r} = \left( \frac{\rho_h}{\rho_c} - 1 \right) 2f \frac{J_1(|\mathbf{G}|r_0)}{|\mathbf{G}|r_0}, \quad \text{for } \mathbf{G} \neq 0, \quad (8)$$

where the integration extends over the two-dimensional unit cell,  $J_1(x)$  is the Bessel function of the first kind, and  $f = \pi(r_0/a)^2$  is the filling fraction. Exactly the same expressions follow for the coefficients of bulk modulus  $b_{\mathbf{G}}^{-1}$ , since the expansion has an analogous form.

In terms of the coefficients of the previous expansions, Eq. (3) becomes

$$\sum_{\mathbf{G}'} [\omega^2 b_{\mathbf{G}-\mathbf{G}'}^{-1} - \rho_{\mathbf{G}-\mathbf{G}'}^{-1} (\mathbf{k} + \mathbf{G}) \cdot (\mathbf{k} + \mathbf{G}')] p_{\mathbf{G}'} = 0. \quad (9)$$

Equation (9) has been numerically solved considering 361 plane waves in the expansion. The number of plane waves has been chosen in order to ensure convergence. Figure 2 shows the band structure for a square lattice of steel cylinders ( $\rho_c = 7.8 \times 10^3$  kg m<sup>-3</sup>,  $B_c = 160 \times 10^9$  N m<sup>-2</sup>) immersed in water ( $\rho_h = 10^3$  kg m<sup>-3</sup>,  $B_h = 2.2 \times 10^9$  N m<sup>-2</sup>). The dimensionless (reduced) frequency  $\Omega = \omega a / 2\pi c_h$  is plotted in terms of the dimensionless wave number of Bloch vector  $\mathbf{K} = \mathbf{k}a / 2\pi$ .

From the solutions of Eq. (9) we can also compute the isofrequency contours. In Fig. 3 the results for the first and second bands are shown. In both cases, the curves show a transition from convex to concave at a particular frequency. The isofrequency contours at the transition point acquire, as shown in the figure, the form of squares with rounded corners. Consequently, there exist locally flat segments of the curve, where, in other words, the spreading of the beam will be counteracted by the crystal anisotropy. Similarly as for photonic crystals in optics the nondiffractive propagation occurs along the diagonals of squares in the first propagation band and along the principal vectors of the lattices in the second band. The “rounded nondiffractive square” is situated

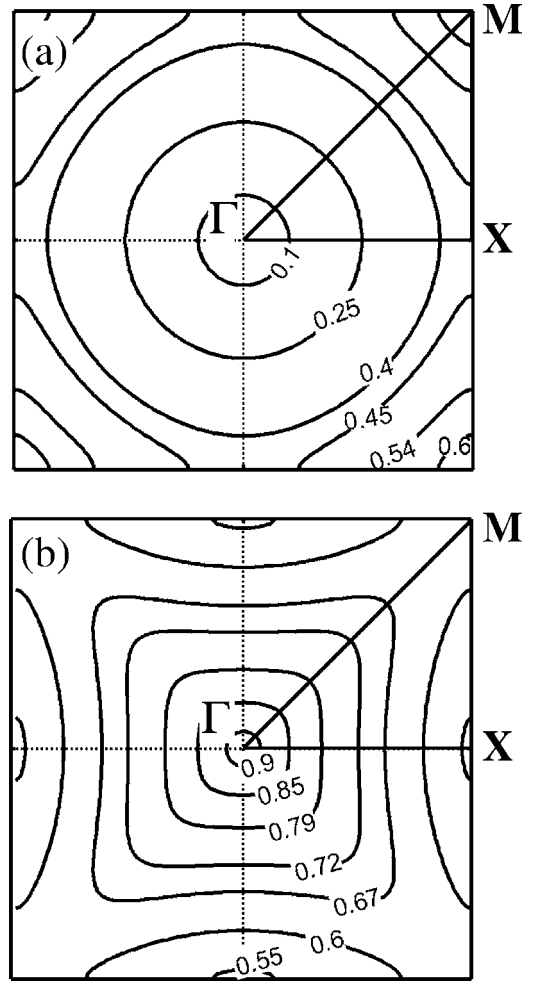


FIG. 3. Isofrequency lines, evaluated for  $a = 5.25$  mm and  $r = 1$  mm, for the first (a) and second (b) bands, centered at the  $\Gamma$  point, as calculated by the expansion into Bloch modes (4)–(7).

around the corner of Brillouin zone (denoted by  $M$ ) for the first band and around the center of the Brillouin zone (denoted by  $\Gamma$ ) in the second band.

### III. NUMERICAL RESULTS

In order to prove the nondiffractive propagation of sound in the sonic crystal, Eqs. (1) have been numerically integrated using the finite-difference time-domain method. The FDTD method is nowadays a standard technique<sup>13</sup> for solving partial differential equations by integrating in time and by approximating the spatial derivatives by finite differences. The incident acoustic beam has been simulated by a plane vibrating surface radiating a harmonic wave with variable frequency  $\omega$ , describing an acoustic transducer with a diameter of 3 cm. The front face of the crystal is located close to the source, where the wave front is nearly plane. The medium parameters were chosen to correspond to numerically evaluated zero diffraction point (by inspecting the isofrequency curves) in the previous section. For the first band [Fig. 3(a)] the isofrequency curve becomes locally flat for  $\Omega \approx 0.54$ , which corresponds to a real frequency of  $\nu$

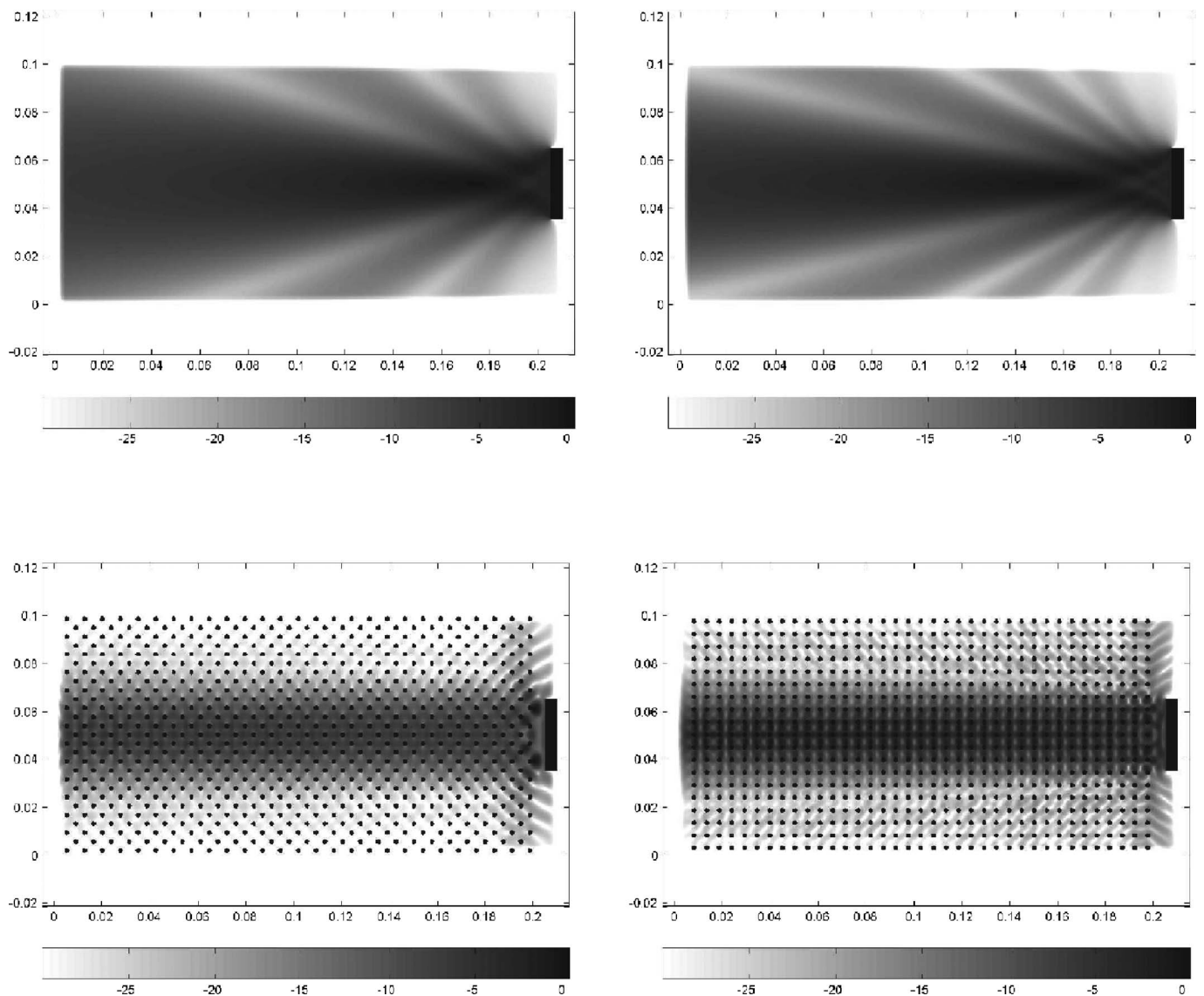


FIG. 4. Numerical FDTD simulation of the nondiffractive beam, for the first two bands. Upper row corresponds to the field radiated by the source without crystal, lower row to the nondiffractive propagation in the [1,1] (left) and [1,0] (right) directions, at the frequencies equal to  $\nu=154$  kHz and  $\nu=217$  kHz as predicted by the theory. Gray levels are in decibel scale and the coordinates in meters. The other parameters are as in Figs. 2 and 3; i.e., steel cylinders in water are simulated with  $r=1$  mm and  $a=5.25$  mm.

$=\Omega c_p/a \approx 154$  kHz and for an incidence along the [1,1] direction. Under these conditions, nondiffractive propagation is predicted to occur. The result of the numerical simulation for these parameters is shown in Fig. 4 (left column). As expected, the beam propagates through the crystal without a visible divergence. For the second band, the theory predicts that the frequency for nondiffractive propagation increases roughly by a factor of  $\sqrt{2}$  with respect to the first band and then occurs at  $\nu \approx 217$  kHz.

We note that whereas the beam in homogeneous media broadens sensibly over the propagation distance, the same beam in the sonic crystal propagates without sensible broadening over much longer distances. Diffractive broadening in a homogeneous medium is quantified by the Rayleigh distance  $L_d=ka^2/2$ , where  $a$  is the radius of the source and corresponds to the distance from the source after which the beam broadens by a factor of  $\sqrt{2}$ . For the two nondiffractive

frequencies evaluated above, the Rayleigh distances are 7.3 cm for the first case and 10.3 cm for the second case.

#### IV. ANALYTICS FOR NONDIFFRACTING BEAMS

The precise analysis of an arbitrary field structure inside the crystal can only be performed by considering the field expansion into an infinite set of modes of the crystal (as stated by the Bloch theorem). The form given by Eqs. (4)–(6) must be assumed, whose unknown amplitudes can be numerically evaluated. This is the basics of the PWE method used in Sec. II for evaluate the band structure and dispersion curves of the crystal. However, it is possible to develop an analytical theory if we consider the particular case of a nondiffractive beam, since this nondiffractive solution appears mainly due to the coupling of three modes, the homogeneous one and the next low-order modes. This situation is illus-

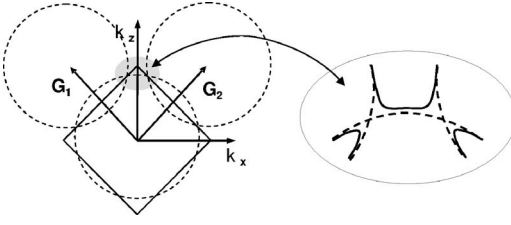


FIG. 5. Schematic picture showing the nondiffractive region (shaded area) resulting from the interaction of three modes. The square represents the limits of the first Brillouin zone. The inset illustrates the lift of the degeneracy at the cross sections of the dispersion curves and the formation of the Bloch modes. The upper Bloch mode can develop flat segments depending on the interaction strength, as the degree of the lift of degeneracy is proportional to the interaction strength.

trated in Fig. 5, where the three intersecting circles, corresponding to the spatial dispersion curves of the three modes (those with wave numbers  $\mathbf{k}$ ,  $\mathbf{k}+\mathbf{G}_1$ , and  $\mathbf{k}+\mathbf{G}_2$ ) give rise to the nondiffractive effect. Due to the interaction between the different spatial modes, the degeneracy at the intersections of the spatial dispersion curves is lifted and the flat areas in the dispersion curve can develop. The radiation belonging to these interacting modes is the most relevant for the deformation of the dispersion curves and to the appearance of the flat segments—i.e., is responsible for the nondiffractive propagation. Therefore the other modes are irrelevant in the “nondiffractive” area (shaded region in Fig. 5), and the Bloch expansion can be simplified as

$$p(\mathbf{r}) = (p_0 + p_1 e^{i\mathbf{G}_1 \cdot \mathbf{r}} + p_2 e^{i\mathbf{G}_2 \cdot \mathbf{r}}), \quad (10)$$

where  $\mathbf{G}_1$  and  $\mathbf{G}_2$  are the basis vectors of the reciprocal space.

Note that since the nondiffractive beam is expected to be highly directive, only  $\mathbf{G}$  vectors directed to the same direction as the wave vector  $\mathbf{k}$  are relevant in the analysis. The material parameters (being real functions) must be, however,

expanded into at least five modes. In particular, the inverses of density and bulk modulus will be assumed to be of the form

$$\bar{\rho}(\mathbf{r})^{-1} = (\rho_0 + \rho_{+1} e^{i\mathbf{G}_1 \cdot \mathbf{r}} + \rho_{+2} e^{i\mathbf{G}_2 \cdot \mathbf{r}} + \rho_{-1} e^{-i\mathbf{G}_1 \cdot \mathbf{r}} + \rho_{-2} e^{-i\mathbf{G}_2 \cdot \mathbf{r}}), \quad (11a)$$

$$\bar{B}(\mathbf{r})^{-1} = (b_0 + b_{+1} e^{i\mathbf{G}_1 \cdot \mathbf{r}} + b_{+2} e^{i\mathbf{G}_2 \cdot \mathbf{r}} + b_{-1} e^{-i\mathbf{G}_1 \cdot \mathbf{r}} + b_{-2} e^{-i\mathbf{G}_2 \cdot \mathbf{r}}), \quad (11b)$$

where the notation  $\rho_{\pm j} = \rho_{\pm \mathbf{G}_j}$ , with  $j=1,2$ , has been used. Substituting Eqs. (11) into Eq. (3) and collecting the terms at the same exponents (those with wave vectors  $\mathbf{k}$ ,  $\mathbf{k}+\mathbf{G}_1$  and  $\mathbf{k}+\mathbf{G}_2$ ), we obtain the following coupled equation system:

$$0 = \omega^2(p_0 b_0 + p_1 b_{-1} + p_2 b_{-2}) - \mathbf{k}^2 p_0 \rho_0 - \mathbf{k}(\mathbf{k} + \mathbf{G}_1) p_1 \rho_{-1} - \mathbf{k}(\mathbf{k} + \mathbf{G}_2) p_2 \rho_{-2}, \quad (12a)$$

$$0 = \omega^2(p_1 b_0 + p_0 b_{+1}) - (\mathbf{k} + \mathbf{G}_1)^2 p_1 \rho_0 - \mathbf{k}(\mathbf{k} + \mathbf{G}_1) p_0 \rho_{+1}, \quad (12b)$$

$$0 = \omega^2(p_2 b_0 + p_0 b_{+2}) - (\mathbf{k} + \mathbf{G}_2)^2 p_2 \rho_0 - \mathbf{k}(\mathbf{k} + \mathbf{G}_2) p_0 \rho_{+2}. \quad (12c)$$

Equations (12) are still too complex to lead to analytical results. However, for small values of the filling fraction  $f$  the solid inclusions can be considered as a perturbation of the homogeneous fluid medium and an asymptotic analysis near the band gap is justified. Next we show that, in this limit, it is possible to obtain a simple relation between the frequency and wave number of the nondiffractive beam and the filling fraction  $f$  characterizing the crystal.

First, note that in the case of small  $f$  (i.e., when  $r_0 \ll a$ ) and materials with high contrast, where  $\rho_h \ll \rho_c$  and  $B_h \ll B_c$  (as occurs, e.g., for steel cylinders in water), the coefficients of the medium expansions in Eqs. (7) and (8) simplify to  $\rho_0 = b_0 = 1 - f$  and  $\rho_i = b_i = -f$ , for  $i = \pm 1, \pm 2$ . Then, Eqs. (12), expressed in matrix form, read

$$\begin{pmatrix} (1-f)(\omega^2 - \mathbf{k}^2) & f[\mathbf{k}(\mathbf{k} + \mathbf{G}_1) - \omega^2] & f[\mathbf{k}(\mathbf{k} + \mathbf{G}_2) - \omega^2] \\ f[\mathbf{k}(\mathbf{k} + \mathbf{G}_1) - \omega^2] & (1-f)[\omega^2 - (\mathbf{k} + \mathbf{G}_1)^2] & 0 \\ f[\mathbf{k}(\mathbf{k} + \mathbf{G}_2) - \omega^2] & 0 & (1-f)[\omega^2 - (\mathbf{k} + \mathbf{G}_2)^2] \end{pmatrix} \begin{pmatrix} p_0 \\ p_1 \\ p_2 \end{pmatrix} = 0. \quad (13)$$

The aim is to obtain the values of  $\omega$  and  $\mathbf{k}$  for which the beam propagates without diffraction. For a crystal with square symmetry, the direction of the nondiffractive propagation with respect the crystal axes can be obtained from the isofrequency curves evaluated in Sec. II. For the first band [Figs. 3(a) and 4] nondiffractive propagation occurs for beams propagating at  $45^\circ$  with respect to the crystal axes—i.e., in the  $^{1,1}$  direction. For our analysis, is convenient to consider the beam axis to be coincident with the  $z$  direction and define a set of unitary basis vectors as  $\mathbf{G}_1 = (-1, 1)/\sqrt{2}$

and  $\mathbf{G}_2 = (1, 1)/\sqrt{2}$ . In this way, all magnitudes in reciprocal space are normalized by  $\pi/a$ .

For small  $f$ , one also expects that the parameters corresponding to the nondiffractive regime take values close to those in the band gap (near the corner of the first Brillouin zone; see Fig. 2). The wave number corresponding to the first band gap is then  $\mathbf{K}_B = (0, 1)/\sqrt{2}$  (recall that, in normalized reciprocal space,  $\mathbf{K} = \mathbf{k}a/2\pi$ ). In order to investigate the behavior of dispersion curves close to this point, we consider waves with wave vector  $\mathbf{K} = \mathbf{K}_B(1 - \delta\mathbf{K})$  with  $\delta\mathbf{K}$

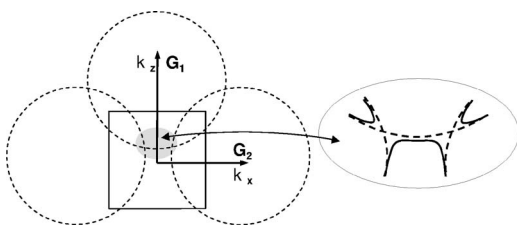


FIG. 6. Schematic picture showing the nondiffractive region (shaded area) in the second propagation band. Everything as in Fig. 5. Here the most relevant modes are  $\mathbf{k} + \mathbf{G}_1$  and  $\mathbf{k} \pm \mathbf{G}_2$ .

$= (\delta K_x, \delta K_z)$  representing small deviations. We further assume that the frequency is close to (but less than) that corresponding to the band gap,  $\Omega = \Omega_B(1 - \delta\Omega)$ , with the normalized gap frequency given by  $\Omega_B = 1/\sqrt{2}$ .

The solvability condition of Eq. (13) results from equating to zero the determinant of the matrix and leads to the relation in the form  $F(\delta\Omega, \delta K_z, \delta K_x; f) = 0$ . Expanding for small  $\delta\mathbf{K} = (\delta K_z, \delta K_x)$ , an analytical transversal dispersion relation  $\delta K_z(\delta K_x)$  is obtained, which allows one to calculate the diffraction coefficient as the curvature of the transverse dispersion curve—i.e.,  $D = (1/2)\partial^2 \delta K_z / \partial \delta K_x^2$ . The nondiffractive point corresponds to  $D = 0$ . This expression is analytical but still cumbersome. However, assuming that  $f \sim O(\varepsilon^2)$  and  $\delta\Omega \sim O(\varepsilon)$ , where  $\varepsilon$  is a smallness parameter, the following simple analytical relation is obtained at the leading order:

$$\delta\Omega_{ND}^{(1)} = f^{2/3} + O(f^{4/3}). \quad (14)$$

Also the wave number of the nondiffractive beam can be analytically evaluated. Substituting Eq. (14) into the solvability condition of Eq. (13) and assuming the above smallness conditions, it follows that

$$\delta K_{ND}^{(1)} = f^{2/3} - f^{4/3} + \frac{3}{4}f^2 + O(f^{7/3}). \quad (15)$$

For the second band, a similar analysis can be performed. The three-mode expansion is illustrated in Fig. 6. In this case it is more convenient to use the vector basis  $\mathbf{G}_1 = (1, 0)$  and  $\mathbf{G}_2 = (0, 1)$ , and now the nondiffractive beam propagation occurs in a direction coincident with one of the lattice vectors. The parameters of the gap are in this case  $\mathbf{K}_B = (1, 0)$  and  $\Omega_B = 1$ . An asymptotic analysis similar to that performed above for the first band shows that  $\delta\Omega_{ND}^{(2)} = \delta\Omega_{ND}^{(1)}$  and  $\delta\mathbf{K}_{ND}^{(2)} = \delta\mathbf{K}_{ND}^{(1)}$ . Then, from the analytics follows that, under the limit of the weak modulation that  $f \sim O(\varepsilon^2)$  and  $\delta\Omega \sim O(\varepsilon)$ , the zero diffraction points for both bands are situated equally, however with respect to the corresponding band gap: the diffraction in the first band disappears just below the first band gap (by  $\delta\Omega_{ND} = f^{2/3}$ ) and in the second band just below the second band gap by the same value (by  $\delta\Omega_{ND}$ ). The wave vector shifts are also equal for both cases. As a consequence, Eqs. (14) and (15) are valid for both bands.

These analytical predictions have been checked numerically. In Fig. 7 the analytical results given by Eqs. (14) and (15) are compared with the corresponding numerical results

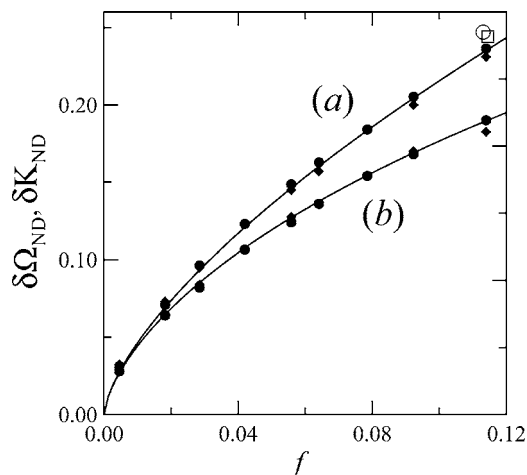


FIG. 7. Dependence of the frequency (a) and wave number of nondiffractive beam, measured with respect to the band gap values, as results from numerical calculation (symbols) and the analytical expressions given in Eqs. (14) and (15). The open circles and squares correspond to the parameter values used for FDTD calculation of nondiffractive propagation (Fig. 4) in the first and second bands, respectively.

(with symbols) obtained with the PWE method using 361 modes. The curve labeled (a) corresponds to the normalized frequency shift, measured with respect to the band gap, and the curve labeled (b) to the wave number shift, for zero diffraction point in the first band (circles) and the second band (squares). The simple expressions obtained under the three-mode expansions are in very good agreement with the numerical results, even for moderate (not very small) values of the filling factor  $f$ .

## V. CONCLUSIONS

Concluding, we have demonstrated theoretically the possibility of nondiffractive propagation of acoustic beams through sonic crystals. We show nondiffractive propagation for both propagation bands: for the first band, where the nondiffractive propagation occurs along the diagonals of the lattice, and for the second band, where diffraction disappears along the principal vectors of the lattice. The diffraction disappears for frequencies just below the corresponding band gaps, with equal frequency shift for both cases given, for not large values of the filling ratio, by a universal and very simple expression  $\delta\Omega_{ND} = f^{2/3}$ .

Relation (15), for the shift of the wave number, which in simplified form reads  $\delta k_{ND} = f^{2/3}$ , allows one to evaluate the width of the nondiffractively propagating beams. Indeed the half-width of the plateau of spatial dispersion curve is roughly equal to (slightly less than)  $\delta k_{ND}$ . This means that beams with normalized size  $d \approx 2\pi / \delta k_{ND} \approx 2\pi f^{-2/3}$  can propagate nondiffractively over large distances (comparing with the diffraction length of the corresponding beam in the homogeneous materials). In terms of nonnormalized coordinates, the minimum size of the beam corresponds to  $d$

$\approx \sqrt{2}af^{-2/3}$ . For a filling factor  $f=0.114$ , corresponding to the numerical simulation in Fig. 4, the width of the nondiffractive beam predicted by this expression results in  $d \approx 6a$ —i.e., in six spatial periods of the lattice. This result is in good agreement with the width of the beam observed in Fig. 4.

## ACKNOWLEDGMENTS

The work has been partially supported by Projects Nos. FIS2005-07931-C03-01 and -03 of the Spanish Ministry of Science and Technology.

- 
- <sup>1</sup>E. Yablonovitch, Phys. Rev. Lett. **58**, 2059 (1987); S. John, *ibid.* **58**, 2486 (1987).  
<sup>2</sup>See, e.g., *Photonic Band Gaps and Localization*, edited by C. M. Soukoulis, Vol. 308 of *NATO Advanced Studies Institute, Series B: Physics* (Plenum, New York, 1993).  
<sup>3</sup>M. Scalora *et al.*, Phys. Rev. E **54**, R1078 (1996); A. Imhof, W. L. Vos, R. Sprik, and A. Lagendijk, Opt. Express **4**, 167 (1999).  
<sup>4</sup>T. Miyashita, Meas. Sci. Technol. **16**, R47 (2005); J. H. Page *et al.*, Phys. Status Solidi B **241**, 3454 (2004).  
<sup>5</sup>R. Morandotti, H. S. Eisenberg, Y. Silberberg, M. Sorel, and J. S. Aitchison, Phys. Rev. Lett. **86**, 3296 (2001); M. J. Ablowitz and Z. H. Musslimani, *ibid.* **87**, 254102 (2001).  
<sup>6</sup>Suxia Yang, J. H. Page, Z. Lin, M. L. Cowan, C. T. Chan, and P. Sheng, Phys. Rev. Lett. **93**, 024301 (2004); M. Torres and F. R. Montero de Espinosa, Ultramicroscopy **42**, 787 (2004).  
<sup>7</sup>E. A. Ostrovskaya and Yu. S. Kivshar, Phys. Rev. Lett. **90**, 160407 (2003); C. Conti and S. Trillo, *ibid.* **92**, 120404 (2004).  
<sup>8</sup>H. Kosaka *et al.*, Appl. Phys. Lett. **74**, 1212 (1999).  
<sup>9</sup>R. Iliew *et al.*, Appl. Phys. Lett. **85**, 5854 (2004); D. W. Prather *et al.*, Opt. Lett. **29**, 50 (2004).  
<sup>10</sup>T. P. White, C. Martijn de Sterke, R. C. McPhedran, and L. C. Botten, Appl. Phys. Lett. **87**, 111107 (2005).  
<sup>11</sup>D. Chigrin, S. Enoch, C. Sotomayor Torres, and G. Tayeb, Opt. Express **11**, 1203 (2003); K. Staliunas and R. Herrero, Phys. Rev. E **73**, 016601 (2006).  
<sup>12</sup>M. S. Kushwaha and P. Halevi, Appl. Phys. Lett. **69**, 31 (1996).  
<sup>13</sup>J. O. Vasseur *et al.*, J. Phys.: Condens. Matter **6**, 8759 (1994).